Evaluation of viscoelastic master curves of filled elastomers and applications to fracture mechanics

2009 J. Phys.: Condens. Matter 21 035104

(http://iopscience.iop.org/0953-8984/21/3/035104)

IOP PUBLISHING JOURNAL OF PHYSICS: CONDENSED MATTER

J. Phys.: Condens. Matter **21** (2009) 035104 (10pp) doi:10.1088/0953-8984/21/3/035104

Evaluation of viscoelastic master curves of filled elastomers and applications to fracture mechanics

M Klüppel

Deutsches Institut für Kautschuktechnologie e.V., Eupener Straße 33, D-30519 Hannover, Germany

E-mail: Manfred.Klueppel@DIKautschuk.de

Received 7 August 2008, in final form 17 September 2008
Published 10 December 2008
Online at stacks.iop.org/JPhysCM/21/035104

Abstract

The viscoelastic response of filler-reinforced elastomers has been investigated by dielectric- and dynamic-mechanical spectroscopy. Horizontal and vertical shifting factors are evaluated, which are used for the construction of viscoelastic master curves. They are discussed in the framework of filler network effects and the slowed-down dynamics of a polymer layer close to the filler surface. The observed shifting behaviour is shown to be related to the superposition of two relaxation processes, i.e. that of the polymer matrix and the filler network, leading to a failure of the time–temperature superposition principle. While the matrix transforms according to the Vogel–Fulcher equation, the filler network exhibits an Arrhenius dependence, which results from the thermal activation of filler–filler bonds, i.e. glassy-like polymer bridges between adjacent filler particles. Based on the viscoelastic master curves relaxation time spectra are evaluated. By referring to a recently developed theory of crack propagation in viscoelastic solids it is demonstrated that the behaviour of the scaling exponent of the relaxation time spectra correlates fairly well with that of the crack propagation rates measured under moderate severity conditions.

(Some figures in this article are in colour only in the electronic version)

1. Introduction

Reinforcement of elastomers by active fillers like carbon black or silica plays an important role in improving the technological potential of rubber goods. In particular, the dynamic properties of tyres at high frequencies, e.g. rolling resistance and wet traction, could be improved significantly by the incorporation of precipitated silica in tyre treads, delivering the so-called green tyre [1, 2]. This new generation of high performance tyres was developed by referring to an *in situ* activation of the silica surface by multifunctional silanes, allowing for an effective dispersibility of the nanoparticles as well as a chemical coupling of the polymer chains to the silica surface. By this technique the poor interaction between the almost non-polar polymer chains and the polar silica surface could be improved and reasonable wear and fracture mechanical properties of the tyre tread could be realized. Nevertheless, a further optimization of the green tyre performance by tailor-made polymer–filler couplings is of great technological interest. Therefore, a fundamental physical understanding of the viscoelastic properties of heterogeneous elastomer materials on a broad frequency scale is required, which also focuses on a detailed knowledge about the influence of reinforcing fillers on the chain mobility during the structural glass transition of polymer nanocomposites. For carbon-black-filled elastomers large dispersive interactions of the chains with the filler imply a strong polymer–filler coupling, leading to an immobilized polymer layer and a gradient of mobility close to the filler surface. In particular, this has been revealed by NMR techniques [3–5]. Nevertheless, it is not clear how the slowed-down chain dynamics at the interface impacts the viscoelastic response of filled elastomers, relevant, for example, for the traction and wear or fracture mechanical properties of tyres, which are know to be strongly affected by the low temperature or high frequency dynamics of the composites [6, 7].

Besides the reduced chain mobility due to attractive interactions, an enhanced mobility of polymer chains at a free surface or repulsive wall in bulk polymers and thin

Table 1. List of ingredients (in phr) of the rubber samples used for experimental investigations.

	Polymers		Fillers						Curatives		
Sample	EPDM	S-SBR	CB	Silica	Silane (Si69)	ZnO	Stearic acid	IPPD	DPG	CBS	S
S-SBR		100				3	1	1.5		2.5	1.7
EPDM	100					3	1	1.5	1.5	2.5	1.7
S60N3		100	60 N339			3	1	1.5		2.5	1.7
S60N5		100	60 N550			3	1	1.5		2.5	1.7
S20K		100		20	1.7	3	1	1.5		2.5	1.7
S40K		100		40	3.3	3	1	1.5		2.5	1.7
S60K		100		60	5	3	1	1.5		2.5	1.7
E60N5	100		60 N550			3	1	1.5	1.5	2.5	1.7

films has been found by experimental techniques [8–11] as well as computer simulations [12]. Long and Lequeux [13] proposed a strongly heterogeneous dynamics of the glass transition and described it by a percolation transition of nanoscopic domains of slow dynamics. In particular, this model allows for an explanation of the variation of the glass transition temperature of thin films both for attractive as well as repulsive interactions and may also explain variations of the glass transition in polymer nanocomposites. For silica–PDMS nanocomposites, a small shift to larger glass transition temperatures has been detected by DSC measurements, accompanied by a broadening of the glass peak on the high temperature side [14, 15]. For carbon black or silica-reinforced technical elastomers, i.e. sulfur cured, filled diene rubbers, dynamic-mechanical measurements indicate no significant shift of the glass transition temperature, but a broadening of the glass transition mainly on the high temperature side is normally observed [7, 16, 20]. This has been explained by the temperature-dependent localization of polymer chain modes close to the strongly attractive filler surface [17]. Furthermore, in these systems an Arrhenius-like increase of the storage modulus with decreasing temperature, appearing well above the glass transition temperature, is found. There are also strong indications that this effect can be explained by a thermal activation of the filler network leading to a failure of the time–temperature superposition principle during the construction of viscoelastic master curves [7]. However, the same effect has also been related to a successive increase of the layer thickness of immobilized polymer with decreasing temperature while approaching the glass transition from the rubbery plateau side [18].

In the present paper we will address the open questions related to micro-mechanical mechanisms affecting the viscoelastic properties of carbon black and silica-filled elastomers. We will demonstrate how dynamic-mechanical master curves of filled elastomers can be constructed and discuss the results in the framework of filler network effects and an immobilized polymer layer close to the filler surface, respectively. We will show how the formation of a filler network can lead to a failure of the time–temperature superposition principle and how the presence of the filler impacts the relaxation time spectrum. Finally, the behaviour of the scaling exponent of the relaxation time spectra will be related to the scaling exponent of fatigue crack propagation rates under moderate severity conditions. Thereby, we will refer to a recently developed theory of crack propagation in viscoelastic solids.

2. Materials and experimental methods

For experimental investigations unfilled and filled elastomers have been compounded in an industrial type, intermeshing mixer (Werner & Pfleiderer GK 1,5 E). Vulcanization of the samples was performed semi-efficiently with sulfur and accelerator (CBS and DPG) in a heat press up to 90% of the vulcameter torque maximum (T90-time). As reinforcing fillers, two types of carbon black (CB), differing in activity (N339, N550) and variable amounts of silica (GR 7000), together with the coupling agent silane (Si 69), have been used. The basic polymers were a solution-styrene-butadiene rubber (S-SBR) with 50 vol% vinyl and 25 vol% styrene (VSL 5025-0) and an amorphous ethylene–propylene-diene rubber with 55% ethylene and 9% ENB (EPDM; Keltan 512). The glass transition temperatures of the samples were obtained from the G'' maximum of temperature-dependent dynamic measurements at 1 Hz and 0.5% strain amplitude as T_g(S-SBR) $= -14\,^{\circ}$C and T_g(EPDM) $= -50\,^{\circ}$C. In the framework of experimental errors these values were found to be independent of filler concentration. All samples were compounded with the processing additives stearic acid and ZnO and protected against ageing by IPPD. The ingredients are listed in table 1.

Measurements of the dielectric properties of the specimens were performed with a broadband dielectric spectrometer, BDS 40 system (Novocontrol GmbH, Germany), providing a bandwidth from 0.1 Hz to 10 MHz. The measurement geometry was a disc-shaped plate capacitor of 30 mm diameter where the specimen was placed between two gold-plated brace electrodes. The thickness of the sample was approx. 2 mm. Thin gold layers were sputtered onto the flat surfaces of the specimens to ensure electrical contact to the electrode plates.

Dynamic-mechanical measurements were performed in the torsion-rectangular mode with strip specimens of 2 mm thickness and 30 mm length with an ARES Rheometer (Rheometric Scientific). The calibration of the compliance of the rheometer was done every year in the framework of accreditation of the lab equipment. For creating dynamic-mechanical master curves frequency-dependent measurements have been performed at different temperatures between -60 and $+70\,^{\circ}$C in several steps, varying the frequency between

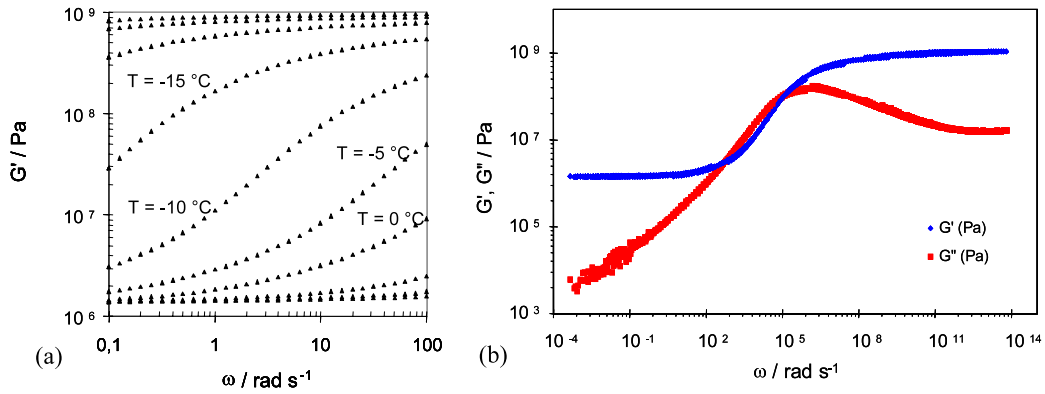

Figure 1. Storage modulus G' versus frequency at 0.5% strain of the unfilled S-SBR sample for various temperatures $T = -30, -25, -20, -15, -10, -5, 0, 10, 20$ and 30 °C (a) and master curves of G' and G'' at $T_{\mathrm{ref}} = 20$ °C after horizontal shifting (b).

0.1 and 100 rad s^{-1}. Thereby, the strain amplitude was kept constant at 0.5%.

Dynamic fracture mechanical investigations were performed on notched strip samples of size 100 mm × 15 mm with a tear fatigue analyzer (TFA) manufactured by Coesfeld, allowing for a fully automatic detection of crack length via a computer-aided optical device. The initial crack length was 1 mm. Measurements were performed in tension mode at room temperature with a small offset stress of 0.1 MPa under harmonic excitation with 4 Hz. The strain was varied between 10% and 35%. To get reasonable statistics the measurements at every strain level were repeated three times. The data scatter of the tear fatigue measurements between different samples of the same type was found to be quite large.

3. Results and discussion

3.1. Evaluation of viscoelastic master curves

While the measurement of the viscoelastic modulus as a function of temperature at a given frequency can be realized on a broad temperature scale, the same mechanical characterization carried out at one temperature by varying the frequency can easily be applied only up to about 100 Hz. The estimation of the high frequency moduli is, however, accessible via the time–temperature superposition principle. It states that the effect of changing the temperature is the same as applying a multiplication factor a_T to the timescale. This concept works well for amorphous, unfilled rubber and allows for the construction of master curves of the complex modulus on a broad frequency scale [23]. This is demonstrated in figure 1 for the unfilled S-SBR sample, where frequency sweeps, performed at different temperatures from 0.1 to 100 rad s^{-1}, are shifted horizontally to obtain master curves for G' and G'' ranging over more than 17 frequency decades. The obtained temperature-dependent horizontal shifting factors a_T will be considered more closely below.

For the construction of viscoelastic master curves of filler-reinforced elastomers it is necessary to evaluate horizontal shifting factors related to the time–temperature superposition of the rubber matrix. This may be done by referring to the horizontal shifting behaviour of the unfilled samples (figure 1). A necessary condition that this shifting procedure works is that the filler does not influence the location of the glass transition. In the case of silica-filled samples, the horizontal shifting factors can also be estimated at the filled sample by measuring the dielectric loss peak during the glass transition on a broad frequency and temperature scale [7, 19, 20]. Thereby, the independence of the location of the glass transition and the horizontal shifting factors from the presence of the filler can be tested. For carbon-black-filled samples this loss peak is normally not detectable, because it is hidden by the pronounced conduction loss of the mobile electrons on the carbon black network.

Figure 2 shows two dielectric loss peaks of the S-SBR sample filled with 60 phr silica (a) and the corresponding activation diagram (b). The low temperature peak can be assigned to fluctuations of a confined layer of water molecules at the silica surface and is denoted 'silica peak'. It can be well described by an Arrhenius behaviour with an activation energy of about 0.6 eV, corresponding to roughly three hydrogen bonds per water molecule, similar to frozen water [21, 22]. The activation energy of the low temperature relaxation transition of confined water is affected by the type of silane used as coupling agent and delivers information about the strength of the polymer–filler coupling, which is discussed elsewhere [21]. The observed high temperature peak is related to the glass transition of the matrix and has been fitted by the semi-empirical Vogel–Fulcher (VF) equation:

$$f = f_\infty \exp\left\{-\frac{E_{\mathrm{A}}}{R\,(T - T_{\mathrm{VF}})}\right\}. \qquad (1)$$

The apparent activation energy $E_{\mathrm{A}} \approx 0.15$ eV obtained from the Vogel–Fulcher fit is much lower than that for confined hydration water and can be assigned to the van der Waals interaction between the polymer chains. The Vogel–Fulcher temperature $T_{\mathrm{VF}} \approx -75$ °C indicates a critical state where the free volume becomes zero. It is found to be about 60 °C below the glass transition temperature $T_{\mathrm{g}} \approx -15$ °C of the S-SBR samples measured by DSC. At the glass transition temperature the free volume becomes too small for a long range, liquid-like segmental mobility and cooperative chain movements are frozen.

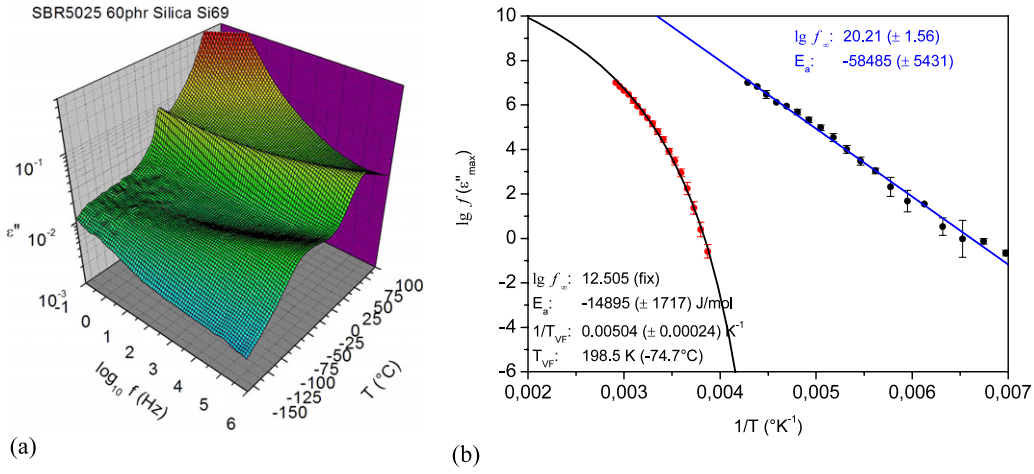

Figure 2. Dielectric loss permittivity of the S-SBR sample filled with 60 phr silica (a) and the corresponding activation diagram (b). Fitting lines with adapted parameters are indicated.

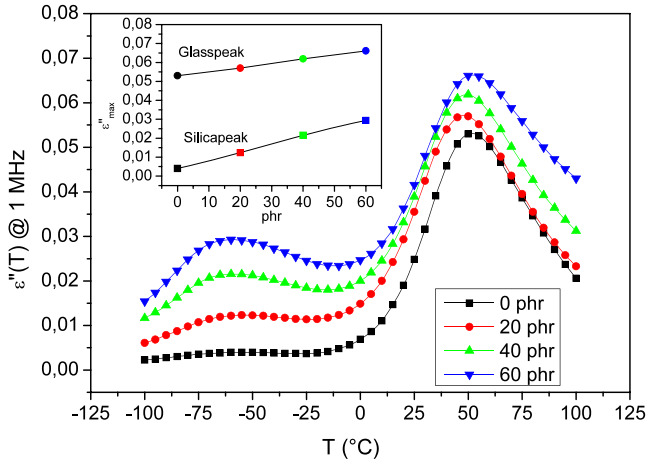

Figure 3. Loss permittivity of the S-SBR composites at 1 MHz versus temperature for different silica concentrations, as indicated; the inset shows the variation of peak heights with silica concentration.

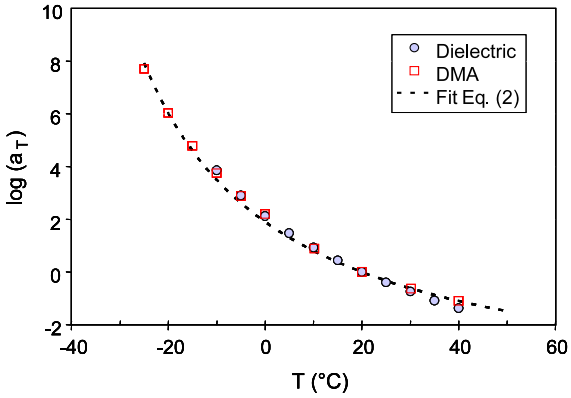

Figure 4. Comparison of horizontal shifting factors ($T_{\rm ref} = 20\,^{\circ}$C) for the unfilled S-SBR sample obtained from dynamic-mechanical analysis (DMA) and dielectric spectroscopy, respectively. The dashed line is a fit of the DMA data with equation (2) giving $C_1 = 7.7$ and $C_2 = 82.7\,^{\circ}$C.

Figure 3 displays the dielectric loss of the S-SBR composites for different silica concentrations at fixed frequency as a function of temperature. It becomes obvious that the location of the glass peak is independent of filler concentration. A similar result is obtained when the location of the loss peaks is compared at smaller frequencies. Furthermore, a systematic broadening of the glass transition with increasing filler concentration is detected. A similar broadening is observed for the loss modulus of various filled elastomers obtained from temperature-dependent dynamic-mechanical measurements [16, 20]. A closer examination shows that this can be related to the slowed-down dynamics of the polymer close to the filler surface, i.e. a gradient of mobility with a layer of immobilized polymer at the silica surface (see below). The inset of figure 3 demonstrates that the height of the 'silica peak' as well as that of the glass peak depend almost linear on the filler volume fraction. From the net increase of the difference of both peaks one can obtain information about the polymer–filler interaction strength, since it impacts the mobility of the water molecule at the silica surface [21].

An equivalent representation to equation (1) for the temperature dependence of relaxation times, which is often used for fitting horizontal shifting factors obtained from dynamic-mechanical analysis (DMA), is given by the Williams–Landel–Ferry (WLF) equation [23]:

$$\log(a_T) = \frac{-C_1(T - T_{\rm ref})}{C_2 + (T - T_{\rm ref})}, \quad \text{for } T_{\rm g} < T < T_{\rm g} + 100\,^{\circ}\text{C}. \tag{2}$$

The two constants C_1 and C_2 are related to the parameters of the Vogel–Fulcher equation (1) and the reference temperature $T_{\rm ref}$ as $C_1 = E_{\rm A}/R(T_{\rm ref} - T_{\rm VF})$ and $C_2 = T_{\rm ref} - T_{\rm VF}$, with R being the gas constant. If the reference temperature is taken as the glass transition temperature, the two constants for many diene rubbers have almost universal values $C_1 = 17.4$ and $C_2 = 51.6\,^{\circ}$C [23].

In figure 4 the temperature-dependent horizontal shifting factors $a_T \equiv \tau(T)/\tau(T_{\rm ref})$ of the unfilled S-SBR samples

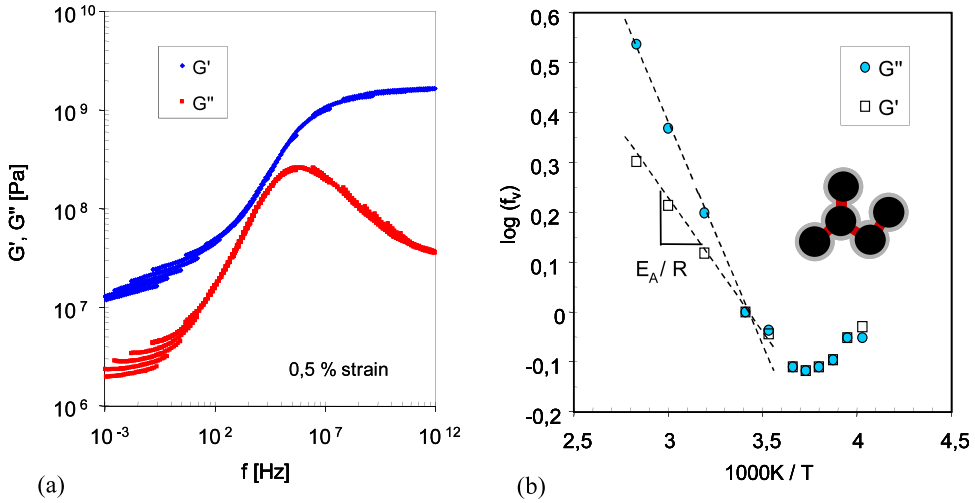

Figure 5. Discontinuous master curves of G' and G'' of the S-SBR sample with 60 phr N339 after horizontal shifting with shift factors from the unfilled sample (a). Arrhenius plot of the vertical shift factors, necessary to get continuous master curves of G' and G'' for the same sample (b). The inset illustrates part of the filler network with glassy-like polymer bridges.

for the reference temperature $T_{\mathrm{ref}} = 20\,^{\circ}\mathrm{C}$ extracted from DMA and dielectric data are compared. They are obtained directly from the horizontal shifting procedure of the dynamic-mechanical moduli depicted in figure 1 and from the location of the dielectric loss peak with the characteristic relaxation time taken as $\tau = 1/f(\varepsilon''_{\mathrm{max}})$, respectively. Figure 4 demonstrates that, in the relevant temperature range, the horizontal shift factors obtained from dynamic-mechanical investigations of the unfilled samples are the same as those obtained from dielectric data. The dashed line shown in figure 4 is a fit of the DMA data with equation (2), giving $C_1 = 7.7$ and $C_2 = 82.7\,^{\circ}\mathrm{C}$. From these values one can evaluate the apparent activation energy $E_{\mathrm{A}} = C_1 C_2 R$, yielding a significantly larger value compared to the one obtained from the Vogel–Fulcher fit in figure 2. However, we point out that this discrepancy has limited physical significance, just demonstrating that the estimated fitting parameters, C_1, C_2, E_{A} and T_{VF}, represent extrapolations of equations (1) and (2) at infinite temperature and relaxation times and, hence, cannot be evaluated very precisely with the limited range of experimental data.

In close correlation of the data depicted in figure 3, we find that the horizontal shift factors, describing the time–temperature superposition of the matrix, are not influenced by the presence of the filler. This becomes clear when the horizontal shifting factors obtained from dielectric data of unfilled and silica-filled samples are compared. In agreement with the findings in [20], one observes that the location of the loss peak is independent of filler concentration and hence the horizontal shift factors are the same for silica-filled and unfilled samples. This indicates that the dielectric loss peak related to the glass transition refers to cooperative movements of the rubber chain backbone and not, for example, that of side groups. Accordingly, the dielectric data can also be used for the evaluation of horizontal shift factors and the construction of viscoelastic master curves for silica-filled samples. As mentioned above, this is not possible for carbon-black-filled samples, because the loss peak is hidden by the pronounced conduction loss of the mobile electrons on the carbon black network.

With the introduction of fillers as reinforcing agents, the complex interactions between the filler network and the polymer matrix leads to a failure of the time–temperature superposition principle. The influence of the filler network during the master procedure can be considered via the introduction of temperature-dependent vertical shift factors f_{V} [7, 20, 24]. Figure 5 illustrates the necessity to introduce vertical shift factors for the low frequency data, corresponding to high temperatures. Indeed, once the isothermal moduli segments are horizontally shifted with the same parameters as for the unfilled system, the poor overlapping in the low frequency region indicates that the time–temperature superposition principle is not fulfilled (figure 5(a)). Overlapping continuous master curves are obtained only if a vertical shifting procedure is applied with different vertical shifting factors for G' and G''. Figure 5(b) demonstrates that, for sufficiently high temperatures, an Arrhenius dependence of the vertical shifting factors f_{V} is well realized. Obviously, the filler system is influencing the dynamic behaviour within the low frequency range and should be associated with a thermally activated mechanism.

We point out that the failure of the time–temperature superposition principle for filled systems is a characteristic viscoelastic effect of the interpenetrating filler network, indicating that the filler network dominates the dynamic-mechanical properties of the composites at small frequencies or high temperatures, because the rubber matrix is softer than the filler network. A similar failure of the time–temperature superposition principle is also well known for heterogeneous polymer blends with interpenetrating phase network morphology if, in a certain frequency or temperature range, only one of the phases is in a glassy state and governs the stiffness of the whole blend system [16]. Accordingly, the physical origin of the complex shifting behaviour in filled elastomers is the superposition of relaxation processes of two

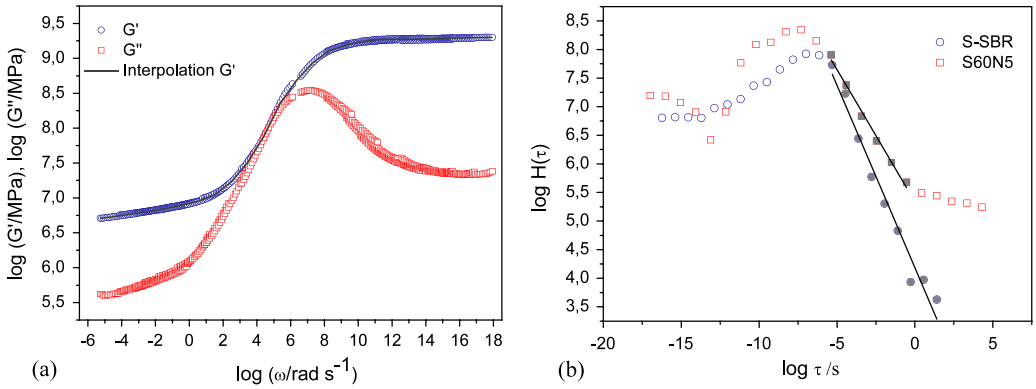

Figure 6. Master curves of G' and G'' at 0.5% strain amplitude of the S-SBR sample S60N5 with 60 phr N550 (a) and corresponding relaxation time spectra for the filled and unfilled S-SBR samples (b). The apparent power law exponents are indicated.

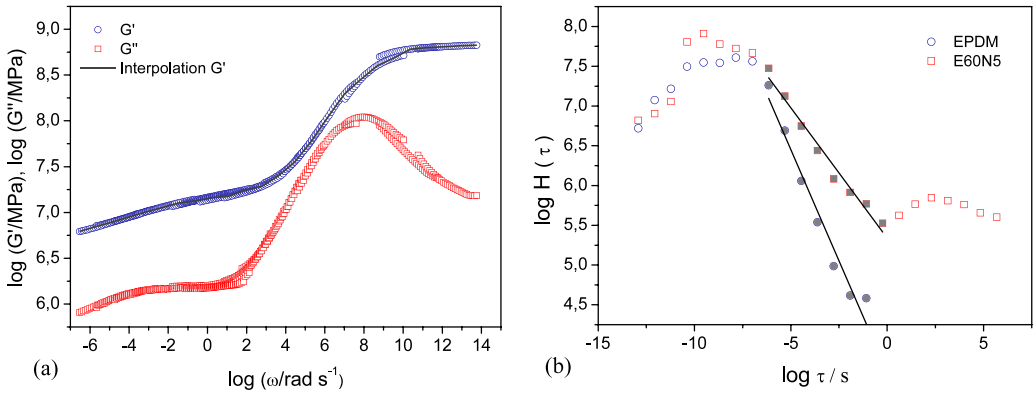

Figure 7. Master curves of G' and G'' at 0.5% strain amplitude of the EPDM sample E60N5 with 60 phr N550 (a) and corresponding relaxation time spectra for the filled and unfilled EPDM samples (b). The apparent power law exponents are indicated.

interpenetrating networks, the polymer and the filler network. While the polymer network transforms according to the Vogel–Fulcher equation (1), the filler network exhibits an Arrhenius dependence. The activation energy of the filler network can be extracted from the vertical shifting factors and corresponds to the thermal activation of the filler–filler bonds, i.e. glassy-like polymer bridges between adjacent filler particles (cf inset of figure 5(b)) [7, 20, 24].

Figure 5 clearly shows that two different activation energies E_A of the filler network can be extracted from the vertical shifting factors of G' and G''. The independent behaviour of G' and G'' can be understood since the evaluation of viscoelastic master curves was carried out at a strain amplitude of 0.5%. This is already in the range of nonlinear response, which starts at very small strain amplitudes around 0.1% [25]. Therefore, the Kramers–Kronig relations are not fulfilled and both components of the dynamic modulus transform independently. Accordingly, G' and G'' transform separately during the application of the vertical shifting procedure. This different behaviour at low frequency also becomes apparent in figure 5(a), whereby the temperature dependence is stronger for the loss modulus G''. By referring to the dynamic flocculation model of rubber reinforcement [24, 26], the two activation processes can be traced back to the thermal activation of two kinds of filler–filler bonds, which become softer with rising temperature. The activation energy associated with G' is related to the stiffness of filler–filler bonds in a virgin state, while the activation energy of G'' corresponds to the stiffness of softer filler–filler bonds in a damaged state, resulting from stress-induced breakdown and re-aggregation of the filler network during cyclic deformations [24].

3.2. Estimation of relaxation time spectra

The role of filler–filler bonds, on the one side, and the slowed-down dynamics close to filler particles, on the other side, in dynamic-mechanical properties can be analysed on different timescales by referring to the spectrum of relaxation times [20]. Accordingly, the relaxation time spectra $H(\tau)$ of the composites have been extracted from the viscoelastic master curves of G' by applying the iterative approximation method of Williams and Ferry [23, 27]:

$$H(\tau) = A\, G' \mathrm{d}\log G'/\mathrm{d}\log\omega\big|_{1/\omega=\tau} \text{ for } p < 1,$$
$$\text{with } A = (2-p)/2\Gamma\left(2-\frac{p}{2}\right)\Gamma\left(1+\frac{p}{2}\right). \qquad (3)$$

Here, p is the local slope of H at $\tau = 1/\omega$, which was found to be smaller than 1 in all cases, and Γ is the gamma function. The results of this evaluation procedure are depicted in figures 6 and 7 for the unfilled S-SBR and EPDM samples

and for the corresponding carbon-black-filled samples S60N5 and E60N5, respectively.

For both polymer types it is found that the presence of carbon black modifies the behaviour of the relaxation time spectrum during the glass transition. As indicated in figures 6(b) and 7(b), a less pronounced drop of relaxation time contributions is observed for the filled systems. For the high-T_g S-SBR samples ($G''_{max} = -14\,°C$), a power law behaviour is more or less realized on timescales between 10^{-6} and 10 s ($H \sim \tau^m$). The scaling exponent increases from $m = -0.64$ for the unfilled to $m = -0.46$ for the filled system. A similar behaviour is observed for the low-T_g EPDM samples ($G''_{max} = -50\,°C$) in the time interval between 10^{-7} and 10^{-1} s. Here, the scaling exponent increases from $m = -0.56$ for the unfilled to $m = -0.33$ for the filled sample. This increase corresponds to the observed broadening of the glass transition on the low frequency or high temperature side and must be assigned to the slowed-down dynamics of the polymer close to the filler surface, implying that, on timescales of the glass transition, the number of non-relaxed dynamic modes decreases less rapidly with time. Accordingly, the observed increase of the scaling exponent m for the filled systems is related to the attractive polymer–filler interaction that hinders the cooperative chain movements close to the filler surface, giving an additional contribution to the relaxation time spectra in the range of the glass transition.

Besides the characteristic power law behaviour of relaxation times in the glass transition regime, figures 6(b) and 7(b) also show a significant contribution of relaxation times of the filled systems for larger times $\tau > 1$ s. For the S-SBR sample S60N5, this looks similar to a second more flat scaling regime with larger power law exponent, while the filled EPDM sample E60N5 exhibits a secondary maximum in the range $1\text{ s} < \tau < 10^5$ s, which correlates with the weak maximum of G'' at low frequencies (figure 7(a)). We argued above that the failure of the time–temperature superposition principle results from the fact that the filler network dominates the viscoelastic properties of the composites in the small frequency regime (cf figure 5(b)). This implies that the relaxation contribution at larger times must be assigned to the filler network. More precisely, we can conclude that the additional contribution to the relaxation time spectrum at large times is related to the viscoelastic properties of the filler–filler bonds, i.e. the glassy-like polymer bridges between adjacent filler particles. The different behaviour of the relaxation time spectra at large time indicates that the morphological and viscoelastic nature of the filler–filler bonds must be different for S-SBR and EPDM composites. Dielectric investigations show that the dc conductivity of carbon-black-filled EPDM is generally larger compared to S-SBR, indicating that the gap size or bond length in EPDM is smaller. Obviously, during flocculation of the filler particles the less tightly adsorbed EPDM chains are squeezed out of the gaps more easily [24]. This leads to stiffer filler–filler bonds, implying that in the small frequency regime the storage modulus of the EPDM sample E60N5 is larger than the corresponding S-SBR sample. This is indeed observed in figures 6(a) and 7(a). Furthermore, it is seen that the frequency dependence of G' in this regime is qualitatively different for the two systems. This again demonstrates that the viscoelastic response of filler–filler bonds in EPDM and S-SBR is generally different.

Table 2. List of fitting parameters of the plots in figure 8 obtained with the power law equation (5) and predicted exponent β^{-1} from the relaxation time spectra and equation (7).

Sample	a [mm^{b+1}/N^b] $\times 10^3$	b	β^{-1}
S-SBR/60phr N550	0.015	2.11	2.85
EPDM/60phr N550	0.01	2.33	2.49
S-SBR (unfilled)	1.0	3.99	3.78
EPDM (unfilled)	0.2	3.23	3.27

3.3. Applications to fatigue crack propagation

In this section we will demonstrate that the scaling exponent m of the relaxation time spectra is closely related to the scaling exponent of fatigue crack propagation rates under moderate severity conditions. The fatigue crack propagation behaviour of the samples has been tested by applying harmonic (sigmoidal) excitations at 4 Hz. For the evaluation of tearing energy, T_{el}, the following semi-empirical equation was used [28]:

$$T_{el} = \frac{2\pi}{\sqrt{\lambda}} W_{el} c. \tag{4}$$

Here, W_{el} is the strain-energy density stored in the specimen far from the crack tip, c is the crack length and λ is the stretch ratio. The elastically stored energy density W_{el} has been estimated by numerical integration of the stress cycles measured on-line for every 100th cycle during the test at the notched samples, whereby the remaining cross section of the sample after subtraction of the crack area was taken as the reference cross section. This approximate evaluation of W_{el} at the notched samples was found to be in good agreement with parallel measurements on samples without a notch. For the determination of fatigue crack propagation rate dc/dn the initial slope of crack length versus cycle number was estimated numerically. Accordingly, the evaluation of data points has been performed only in the range where the crack length is small compared to the sample width.

The fatigue crack propagation properties are normally described by a double-logarithmic plot of fatigue crack propagation rate dc/dn versus tearing energy T_{el}, with T_{el} estimated by equation (4) and n being the number of cycles. This type of power law behaviour is often termed a Paris plot:

$$\frac{dc}{dn} = a T_{el}^b. \tag{5}$$

Figure 8 shows the dependence of fatigue crack propagation rate dc/dn on tearing energy T_{el} for the unfilled EPDM and S-SBR samples and the corresponding filled systems E60N5 and S60N5 with 60 phr N550. The inserted regression lines indicate that equation (5) fits fairly well to the experimental data in the depicted range of tearing energy values. The two fitting parameters a and b are summarized in table 2. It is found that the filled samples exhibit a higher

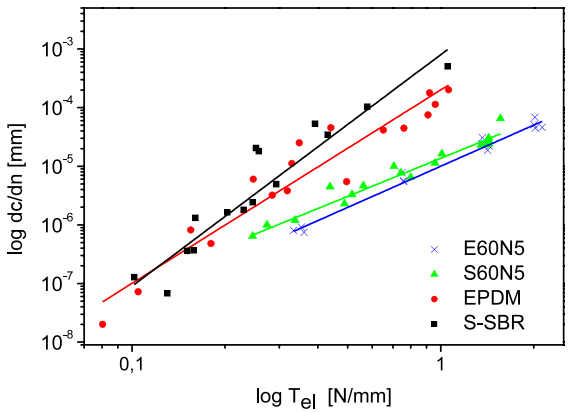

Figure 8. Power law behaviour (lines) of fatigue crack propagation rate versus tearing energy for the unfilled and filled (60 phr N550) EPDM and S-SBR samples under harmonic loading. Solid lines are fits with equation (5).

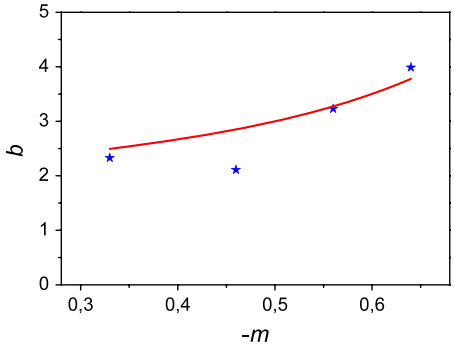

Figure 9. Plot of the power law exponent $-m$ from relaxation time spectra (figures 6, 7) versus b from tear fatigue data (figure 8). The solid line shows the prediction of equation (7) with $\beta^{-1} = b$.

tear resistance and a smaller slope of the regression lines than those for the unfilled systems (cf table 2). Furthermore, the tear resistance of the EPDM systems is higher than that of the S-SBR systems in all cases. For pulsed loading this difference is more significant, since flash temperature effects increase the crack growth rate of the S-SBR more than that of the EPDM due to a higher temperature stability.

Since under harmonic loading flash temperature effects are expected to be small, we can try to relate the fracture mechanical results presented in figure 8 to the viscoelastic properties of the samples depicted in figures 6 and 7. Recently, a theory of crack propagation in viscoelastic solids has been proposed [29, 30]. This theory is based on rate-dependent crack opening mechanisms predicting a trumpet-like shape of the crack contour due to viscoelastic effects [31]. It was initially derived for describing peeling effects of soft adhesives [31] and later was used for the evaluation of the contribution of adhesion to the stationary friction of rubber at rough, rigid substrates [7, 19]. In these models the surface energy $\gamma_{\rm eff}$ is considered to be a rate- or velocity-dependent function that can be well approximated by the following semi-empirical expression [19]:

$$\gamma_{\rm eff} = \gamma_0 \left(1 + \frac{E_\infty/E_0}{(1 + (\upsilon_{\rm c}/\upsilon))^\beta}\right). \tag{6}$$

At low crack opening rates, $\upsilon \ll \upsilon_{\rm c}$, the effective surface energy exhibits a constant value corresponding to the static surface energy γ_0. By increasing the crack opening rate, $\gamma_{\rm eff}$ goes through a step-like transition. The step height of the transition is given by the modulus ratio obtained from dynamic-mechanical measurements, E_∞/E_0, i.e. the ratio of the dynamic moduli in the glassy and rubbery state. According to equation (6), $\gamma_{\rm eff}$ follows a power law with exponent β until a critical velocity $\upsilon_{\rm c}$ is reached ($\gamma_{\rm eff} \sim \upsilon^\beta$). The exponent β is related to the power law exponent m of the relaxation time spectrum ($H \sim \tau^m$):

$$\beta = \frac{1+m}{2+m}. \tag{7}$$

Equation (6) holds for the case of steady crack propagation in viscoelastic solids [29, 30] and cannot directly be applied to fatigue crack propagation under pulsed or harmonic straining. Nevertheless, the typical viscoelastic effects related to the crack opening mechanism should also be present for the second case. Then, the crack velocity υ could be identified with the fatigue crack propagation rate $\mathrm{d}c/\mathrm{d}n$. Accordingly, since the tearing energy equals the double surface energy, $T_{\rm el} = 2\gamma_{\rm eff}$, it is expected to show a characteristic power law behaviour in an intermediate crack velocity regime $\mathrm{d}c/\mathrm{d}n < (\mathrm{d}c/\mathrm{d}n)_{\rm c}$ corresponding to $\upsilon < \upsilon_{\rm c}$:

$$T_{\rm el} \sim \left(\frac{\mathrm{d}c}{\mathrm{d}n}\right)^\beta. \tag{5'}$$

This behaviour is indeed observed in the Paris plots of figure 8, implying that the inverse value of β should equal the fitting parameter b ($\beta^{-1} = b$).

In figures 6 and 7 the relaxation time spectra have been calculated from the viscoelastic moduli of the unfilled and filled (60 phr N550) S-SBR and EPDM samples, respectively. From the obtained power law exponents m one can calculate the crack propagation exponents β^{-1} predicted by equation (7). The resulting values of β^{-1} are listed in the right column of table 2. If these are compared with the fitted exponents b, also listed in table 2, one finds fair agreement between both values. The correlation between both exponents is explicitly shown in figure 9. A significant deviation of about 20% is only observed for the filled S-SBR sample S60N5. This deviation indicates that, beside viscoelastic effects, crack propagation might also be affected by other factors, e.g. the properties of the filler network or the specific heterogeneous structure of the composites. Nevertheless, for the unfilled systems the values of b and β^{-1} agree very well and in both cases systematic lower values are obtained for EPDM compared to S-SBR. Furthermore, the systematically lower values of the exponent, $b \approx 2.33$ and 2.11, for the filled EPDM and S-SBR systems in comparison to the unfilled systems are in qualitative agreement with the predicted lower exponents $\beta^{-1} \approx 2.49$ and 2.85, respectively. Insofar, we can relate the characteristic variation of the power law exponent of the crack propagation rate under moderate severity conditions to the characteristic modification of the power law exponent of the relaxation time spectra.

4. Conclusions

In the present paper the viscoelastic properties of unfilled and filler-reinforced elastomers have been investigated using dielectric and dynamic-mechanical analysis. Based on dynamic-mechanical master curves relaxation time spectra have been evaluated, which were shown to be closely related to fatigue crack propagation rates measured under moderate severity conditions. In particular, the following conclusions can be drawn.

(i) For the construction of dynamic-mechanical master curves of filled elastomers horizontal as well as vertical shifting factors have to be applied. This complex shifting behaviour is related to the superposition of two relaxation processes, i.e. that of the polymer matrix and that of the filler network, leading to a failure of the time–temperature superposition principle. While the polymer matrix transforms according to the Vogel–Fulcher equation, the filler network exhibits an Arrhenius dependence. The activation energy of the filler network can be extracted from the vertical shifting factors and corresponds to the thermal activation of filler–filler bonds, i.e. glassy-like polymer bridges between adjacent filler particles. The activation energy associated with G' is related to the stiffness of filler–filler bonds in a virgin state, while the activation energy of G'' corresponds to the stiffness of softer filler–filler bonds in a damaged state.

(ii) The horizontal shift factors, describing the time–temperature superposition of the polymer matrix, are independent of filler concentration. This holds, since the location of the dielectric loss peak is not influenced by the presence of the filler and the horizontal shift factors estimated from dielectric data are the same as those obtained from the horizontal shifting procedure of the unfilled samples (figures 3 and 4). Accordingly, the horizontal shift factors of the filled systems can be estimated via dynamic-mechanical measurements at the unfilled samples or, in the case of non-conducting silica-filled samples, by measuring the dielectric loss peak during the glass transition on a broad frequency and temperature scale (figures 1 and 2).

(iii) The application of horizontal shifting factors obtained from the unfilled samples for the construction of master curves of the corresponding filled samples leads to a failure of the time–temperature superposition principle in the small frequency regime (figure 5). This must be identified as a characteristic effect of the interpenetrating filler network, indicating that the filler network dominates the viscoelastic properties of the composites at small frequencies or large times.

(iv) For the filled systems, a significant contribution of relaxation times is found in the range of larger times ($1\ \mathrm{s} < \tau < 10^5\ \mathrm{s}$). This contribution is due to the filler network and refers to the specific viscoelastic properties of the filler–filler bonds. The different behaviour of the relaxation time spectra of S-SBR and EPDM composites at large times indicates that the morphological and viscoelastic nature of the filler–filler bonds is different for both systems.

(v) The relaxation time spectra exhibit a power law behaviour on timescales between 10^{-6} and 1 s and the scaling exponent increases from about $m \approx -0.6$ for the unfilled samples to $m \approx -0.4$ for the filled system (figures 6(b) and 7(b)). This increase can be related to the slowed-down dynamics of the polymer close to the filler surface. By referring to a recently developed theory of crack propagation in viscoelastic solids [29, 30] it is demonstrated that the behaviour of the scaling exponent m of the relaxation time spectra correlates fairly well with that of the Paris plots b (crack propagation rates versus tearing energy) obtained under moderate severity conditions (figure 9).

Acknowledgments

This work was supported by the Deutsche Forschungsgemeinschaft (FOR 597). The valuable help of Dr B Bandow (RZ, Hannover), Dipl.-Chem. J Fritzsche (DIK), Dr A Le Gal (Ciba, Basel) and Dr J G Meier (ITA, Zaragoza) during their employment at the DIK is highly appreciated.

References

[1] Wolff S 1993 Silica based tread compounds—background and performance *Proc.: Tire Tech '93 (Basel, Oct.)*
[2] *Patent Application (Michelin) European Patent* 0501 227 *Patent Application (Michelin) US Patent* 5,227,425
[3] Litvinow V M and Stee'mann P A 1999 *Macromolecules* **32** 8476
[4] Dutta N K *et al* 1994 *Polymer* **35** 4293
[5] Lüchow H, Breier E and Gronski W 1997 *Rubber Chem. Technol.* **70** 747
[6] Grosch K A 1996 *Rubber Chem. Technol.* **69** 495
[7] Le Gal A, Yang X and Klüppel M 2005 *J. Chem. Phys.* **123** 014704
[8] Kremer F, Huwe A, Schönhals A and Rozanski S A 2003 *Broadband Dielectric Spectroscopy* ed F Kremer and A Schönhals (Berlin: Springer) chapter 6 (Molecular Dynamics in Confining Space)
[9] Forrest J A, Dalnoki-Veress K, Stevens J R and Dutscher J R 1996 *Phys. Rev. Lett.* **77** 2002
[10] Hartmann L, Fukao K and Kremer F 2003 *Broadband Dielectric Spectroscopy* ed F Kremer and A Schönhals (Berlin: Springer) chapter 11 (Molecular Dynamics in Thin Polymer Films)
[11] Grohens Y, Hamon L, Reiter G, Soldera A and Holl Y 2002 *Eur. Phys. J.* E **8** 217
[12] Starr F W, Schroeder T B and Glotzer S C 2002 *Macromolecules* **35** 4481
[13] Long D and Lequeux F 2001 *Eur. Phys. J.* E **4** 371
[14] Winberg P, Eldrup M and Maurer F H J 2004 *Polymer* **45** 8253
[15] Fragiadakis D, Pissis P and Bokobza L 2005 *Polymer* **46** 6001
[16] Klüppel M, Schuster R H and Schaper J 1999 *Rubber Chem. Technol.* **72** 91
[17] Huber G and Vilgis T A 1998 *Eur. Phys. J.* B **3** 217
[18] Berriot J, Montes H, Lequeux F, Long D and Sotta P 2003 *Europhys. Lett.* **64** 50
Berriot J, Montes H, Lequeux F, Long D and Sotta P 2002 *Macromolecules* **35** 9756
[19] Le Gal A and Klüppel M 2008 *J. Phys.: Condens. Matter* **20** 015007

[20] Fritzsche J and Klüppel M 2008 *Macromol. Rapid Commun.* submitted
[21] Meier J G, Fritzsche J, Guy L, Bomal Y and Klüppel M 2008 *Macromolecules* submitted
[22] Spanoudaki A, Albela B, Bonneviot L and Peyrard M 2005 *Eur. Phys. J.* E **17** 21
[23] Ferry J D 1980 *Viscoelastic Properties of Polymers* 3rd edn (New York: Wiley)
[24] Klüppel M 2003 *Adv. Polym. Sci.* **164** 1
[25] Payne A R 1963 *Rubber Chem. Technol.* **36** 432
[26] Klüppel M, Meier J and Dämgen M 2005 *Constitutive Models for Rubber IV* ed P-E Austrell and L Kari (Rotterdam: Balkema) p 171
[27] Williams M L and Ferry J D 1953 *J. Polym. Sci.* **11** 169
[28] Gent A N 2001 *Engineering with Rubber* 2nd edn (Munich: Hanser Publishers)
[29] Persson B N J and Brener E A 2005 *Phys. Rev.* E **71** 036123
[30] Persson B N J, Ahlbor O, Heinrich G and Ueba H 2005 *J. Phys.: Condens. Matter* **17** R1071
[31] de Gennes P G 1996 *Langmuir* **12** 4497